Materials Science and Engineering C 33 (2013) 699–706

Contents lists available at SciVerse ScienceDirect

Materials Science and Engineering C

journal homepage: www.elsevier.com/locate/msec

Fabrication of mineralized electrospun PLGA and PLGA/gelatin nanofibers and their potential in bone tissue engineering

Z.X. Meng [a], H.F. Li [b], Z.Z. Sun [a], W. Zheng [a,*], Y.F. Zheng [a,b,**]

[a] Center for Biomedical Materials and Engineering, Harbin Engineering University, Harbin 150001, China
[b] Department of Materials Science and Engineering, College of Engineering, Peking University, Beijing 100871, China

ARTICLE INFO

Article history:
Received 23 January 2012
Received in revised form 18 September 2012
Accepted 28 October 2012
Available online 2 November 2012

Keywords:
Electrospinning
Mineralization
Poly(D, L-lactide-co-glycolide)
Gelatin
Calcium phosphate

ABSTRACT

Surface mineralization is an effective method to produce calcium phosphate apatite coating on the surface of bone tissue scaffold which could create an osteophilic environment similar to the natural extracellular matrix for bone cells. In this study, we prepared mineralized poly(D,L-lactide-co-glycolide) (PLGA) and PLGA/gelatin electrospun nanofibers via depositing calcium phosphate apatite coating on the surface of these nanofibers to fabricate bone tissue engineering scaffolds by concentrated simulated body fluid method, supersaturated calcification solution method and alternate soaking method. The apatite products were characterized by the scanning electron microscopy (SEM), Fourier transform-infrared spectroscopy (FT-IR), and X-ray diffractometry (XRD) methods. A large amount of calcium phosphate apatite composed of dicalcium phosphate dihydrate (DCPD), hydroxyapatite (HA) and octacalcium phosphate (OCP) was deposited on the surface of resulting nanofibers in short times via three mineralizing methods. A larger amount of calcium phosphate was deposited on the surface of PLGA/gelatin nanofibers rather than PLGA nanofibers because gelatin acted as nucleation center for the formation of calcium phosphate. The cell culture experiments revealed that the difference of morphology and components of calcium phosphate apatite did not show much influence on the cell adhesion, proliferation and activity.

© 2012 Elsevier B.V. All rights reserved.

1. Introduction

Bone defects are common diseases and the number of patients suffering from this condition keeps increasing. As a conventional treatment, the autogenetic and allogenetic bones are not sufficient for such a number of patients because of their limited supplement [1,2]. Therefore, finding a new substitute for bone regeneration with broad source and low cost is a mission for the researchers. As a promising approach, the substitute of tissue engineering scaffold combined with bone cells is positive for repairing or regenerating the functions of the damaged tissue.

The electrospun nanofiber membrane has been recently used as tissue engineering scaffold to support the adhesion and proliferation of cells, because its structure possesses high surface to volume ratio and high porosity which is similar to the natural extracellular matrix (ECM) [3,4]. Since the calcium phosphate (CaP) apatite such as hydroxyapatite (HA) is similar to the component of bone, the electrospun scaffolds consisted of biodegradable polymers and ceramic nanoparticles of calcium phosphates have obtained great progress in bone tissue engineering [5,6]. However, the electrospun scaffold blended with plenty of calcium phosphate nanoparticles often has low mechanical properties due to the agglomeration of the calcium phosphate nanoparticles. Recently Gupta et al. combined the electrospinning and electrospraying techniques and found that HA nanoparticles sprayed on the surface of the electrospun scaffold could not only enhance the attachment and proliferation of human fetal osteoblasts, but also possess higher mechanical property than that of the electrospun scaffold blended with HA nanoparticles [7]. Thus similar surface mineralization methods have been the major current in the research of bone tissue engineering scaffolds, which could deposit CaP apatite on the surface of the electrospun nanofibers to structure an osteophilic environment for bone cells [8,9]. Compared with general mineralizing method, rapid mineralizing methods such as concentrated simulated body fluid (SBF) method, supersaturated calcification solution method and alternate soaking method possess high efficiency which would decrease the mineralizing time from several days to several hours [10–12]. However, most of these reports focus on the fabrication or characterizations, few of them compare the resemblance or difference of the apatite prepared by these methods.

Poly(D,L-lactide-co-glycolide) (PLGA), as a biodegradable synthetic polymer, has been electrospun into nanofibers and widely been explored in the biomedical field for many years. Due to its excellent biocompatibility, controllable degradation and suitable mechanical property, thus PLGA was selected as mineralized matrix in many researches [13,14]. However, Ngiam et al. found that PLGA/collagen

* Corresponding author.
** Correspondence to: Y.F. Zheng, Department of Materials Science and Engineering, College of Engineering, Peking University, Beijing 100871, China. Tel./fax: +86 10 6276 7411.
E-mail addresses: zhengwei@hrbeu.edu.cn (W. Zheng), yfzheng@pku.edu.cn (Y.F. Zheng).

0928-4931/$ – see front matter © 2012 Elsevier B.V. All rights reserved.
http://dx.doi.org/10.1016/j.msec.2012.10.021

nanofiber could improve the efficiency of mineralization although decreasing the mechanical property, because the carboxyl groups of collagen could enrich Ca^{2+} ions [15]. Gelatin is the partial hydrolyzate of collagen which is also a good biomaterial and has lower cost than collagen. Our previous work found that PLGA/gelatin 9/1 nanofibers possessed higher tensile stress and hydrophilicity than PLGA nanofibers [16]. Therefore, we used the concentrated simulated body fluid method, supersaturated calcification solution method and alternate soaking method, which are the popular rapid mineralizing methods, to form CaP apatite on the surface of PLGA and PLGA/gelatin 9/1 electrospun nanofibrous scaffolds to investigate the resemblance and difference of the morphologies, structures and components of CaP apatite, together with the attachment, proliferation and activity of the MG63 cells on the surface of the mineralized PLGA and PLGA/gelatin 9/1 electrospun scaffolds by scanning electron microscopy (SEM), 3-(4,5-dimethylthiazol-2-yl)-2,5-diphenyltetrazoliumbromide (MTT) assay and alkaline phosphatase (ALP) activity analysis.

2. Materials and method

2.1. Nanofiber preparation

The composite solution with a concentration of 10% w/v was prepared by dissolving PLGA (LA/GA 85/15, M_w = 200,000 Jinan Daigang Biomaterial Co. Ltd., China) and gelatin from swine (Tianjin Bodi Chemical Co. Ltd., China) with the weight ratio of 10/0 and 9/1 in 1,1,1,3,3,3-hexafluoro-2-propanol (Shanghai Jingchun Chemical Regent Co. Ltd. China) under stirring for 12 h at room temperature.

For electrospinning, the composite solution was loaded in a 5 mL plastic syringe and injected through a stainless-steel blunt needle using an infusion pump (TS2-60, Baoding Longer Precision Pump Co. Ltd., China) at an injection rate of 0.5 $mL \cdot h^{-1}$ with an applied voltage of 7 kV (HB-F303-1-AC, China). Nanofibers were collected on a flat collector which was kept at a distance of 10 cm from the needle tip. The scaffolds were dried overnight under vacuum at room temperature.

2.2. Mineralizing process

Method 1: the concentrated SBF solution was similar to Yang's report [10], the reagent of NaCl, KCl, $CaCl_2$, $MgCl_2 \cdot 6H_2O$ and $NaH_2PO_4 \cdot 2H_2O$ was put into the doubly distilled water, after the chemical dissolved completely $NaHCO_3$ was added into the solution. The salt concentration was summarized in Table 1. For mineralizing, the PLGA and PLGA/gelatin nanofibrous scaffolds (20×20 mm^2) were immersed into the fresh concentrated SBF solution for 1–3 h, after that the samples were taken out and washed with doubly distilled water. Subsequently, the samples were first dried in the air overnight and then under vacuum at room temperature for 24 h.

Method 2: the supersaturated calcification solution method was performed according to Liao's report [11]. In brief, the PLGA and PLGA/gelatin scaffolds were immersed into the acetic acid (0.5 $mol \cdot L^{-1}$), subsequently the aqueous solution of $CaCl_2$ (0.5 $mol \cdot L^{-1}$) and H_3PO_4 (0.5 $mol \cdot L^{-1}$) were gradually added at the Ca/P molar ration of 1.67. The mixture solution was stirred continually, titrated with NaOH solution to pH 9, and maintained at room temperature for 1–3 h. After that the samples were first dried in the air overnight and then under vacuum at room temperature for 24 h.

Method 3: the alternate soaking method followed Taguchi's report [12]. Briefly, the PLGA and PLGA/gelatin nanofibrous scaffolds (20×20 mm^2) were immersed into a $CaCl_2$ solution (0.5 $mol \cdot L^{-1}$) for 5 min and then into a Na_2HPO_4 solution (0.5 $mol \cdot L^{-1}$) for 5 min to end one cycle. The cycles were continuing until set times. The samples were rinsed with doubly distilled water after taken out from each solution. The coating process sustained for 1–3 h, and then the samples were first dried in the air overnight and then under vacuum at room temperature for 24 h.

Table 1
Composition of concentrated SBF solution.

Reagent	g/L
NaCl	54.443
KCl	0.373
$CaCl_2$	2.775
$MgCl_2 \cdot 6H_2O$	1.015
$NaH_2PO_4 \cdot 2H_2O$	1.559
$NaHCO_3$	0.840

2.3. Characterization

The morphologies of the mineralized electrospun nanofibers were observed by SEM (CamScan MX2600FE, UK) at an accelerating voltage of 20 kV. All samples were coated with a thin layer of gold in two 30 s consecutive cycles at 45 mA to reduce charging and produce a conductive surface. The energy dispersive spectrum (EDS) was used to examine the elemental constituents of mineralized nanofibers.

The weight increase of electrospun scaffold was calculated by using the following equation:

$$\text{Weight increase } (\%) = \frac{m - m_0}{m_0} \times 100\% \quad (1)$$

where m_0 is the weight of the initial electrospun scaffold, m is the weight of mineralized electrospun scaffold.

FT-IR spectra were recorded for mineralized electrospun scaffolds (mineralizing for 2 h) in the attenuated total reflection (ATR) mode using an IR spectrophotometer (PE Company, USA). The spectra were obtained with 16 scans per sample ranging from 4000 to 650 cm^{-1}.

The components of all the samples (mineralizing for 2 h) were characterized by X-ray diffractometer (FEI Company, USA) equipped with Cu-Kα source and operating at 40 kV and 40 mA. The diffraction patterns were obtained at a scan rate of $5° \cdot min^{-1}$.

2.4. Cell experiment

Human osteosarcoma cell line MG63 (Cell Resource Center of the Chinese Academy of Medical Sciences and Peking Union Medical College) were cultured in minimum essential medium (MEM) with 10% fetal bovine serum (FBS), 100 $U \cdot mL^{-1}$ penicillin and 100 $\mu g \cdot mL^{-1}$ streptomycin. The cell culture was maintained at 37 °C in a humidified incubator containing 5% CO_2 and the medium was changed every day. After reaching 80–90% confluence, the cells were trypsinized and counted with a hemocytometer. The electrospun nanofibrous scaffolds were cut into small slices and placed in the cell culture plate. After sterilization under UV radiation for 2 h, they were rinsed several times with phosphate buffered saline (PBS) and soaked in MEM for 24 h before cell seeding. Subsequently, the cells were seeded on electrospun PLGA, PLGA/gelatin nanofibrous scaffolds and MEM medium containing supplement as a negative control with seeding density of 5000 cells/well, respectively, and were cultured in a humidified atmosphere of 5% CO_2 at 37 °C up to desired time points.

The morphological study of MG63 cells cultured on PLGA and PLGA/gelatin nanofibrous scaffolds were performed by SEM. After 1 and 4 days of cell culture, the cell-cultured scaffolds were processed for SEM studies. The scaffolds were rinsed twice with PBS and fixed in 3% glutaraldehyde for 3 h. Thereafter, the scaffolds were rinsed in double distilled water and dehydrated with upgrading concentrations of ethanol (30%, 50%, 70%, 90%, 100%) for 15 min each. Final washing with 100% ethanol was followed by treating the specimens with hexamethyldisilazane (HMDS). The HMDS was air-dried by keeping the samples in fume hood. Finally the scaffolds were sputter coated with gold and then observed under SEM.

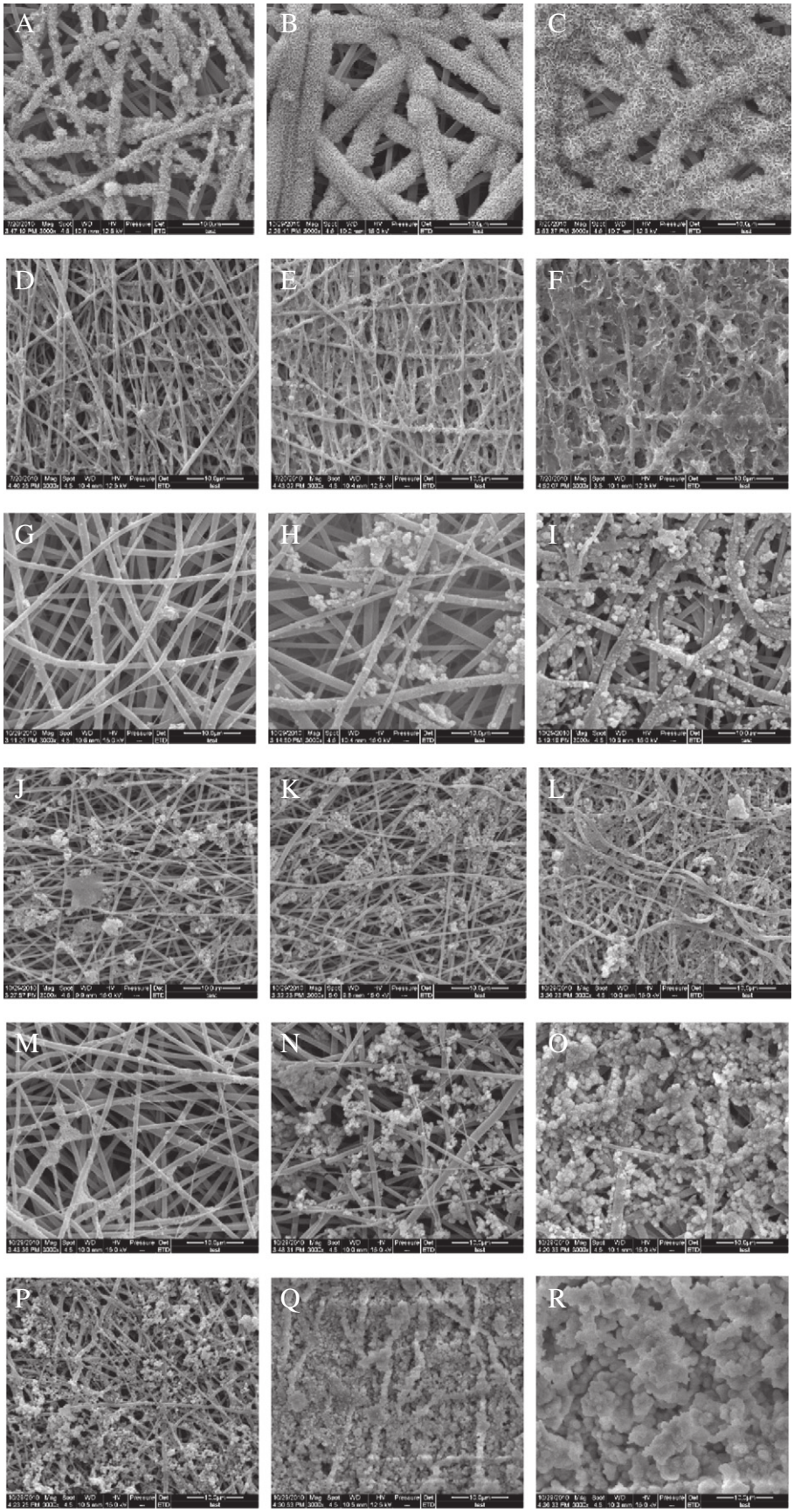

Fig. 1. Morphologies of mineralized PLGA and PLGA/gelatin nanofibers with different soaking times. Concentrated SBF method: PLGA (A) 1 h (B) 2 h (C) 3 h; PLGA/gelatin (D) 1 h (e) 2 h (F) 3 h; Supersaturated calcification solution method: PLGA (G) 1 h (H) 2 h (i) 3 h; PLGA/gelatin (J) 1 h (k) 2 h (L) 3 h; Alternate soaking method: PLGA (M) 1 h (N) 2 h (O) 3 h; PLGA/gelatin (P) 1 h (Q) 2 h and (R) 3 h.

Table 2
Weight increase of mineralized PLGA and PLGA/gelatin nanofibers with different times.

Method	Time (h)	Weight increase (%)	
		PLGA	PLGA/gelatin
Concentrated SBF solution method	1	4.7 ± 1.5	9.6 ± 2.0
	2	12.4 ± 6.8	22.7 ± 9.4
	3	25 ± 10	39 ± 13
Supersaturated calcification solution method	1	1.25 ± 0.84	2.87 ± 0.98
	2	1.90 ± 0.25	6.5 ± 1.1
	3	2.64 ± 0.71	8.6 ± 1.9
Alternate soaking method	1	1.97 ± 0.72	17.9 ± 4.6
	2	15.1 ± 9.8	129 ± 58
	3	168 ± 102	240 ± 164

The cell adhesion and proliferation on the scaffolds were measured by MTT assay. Briefly, after 1, 2 and 4 days, 10 μL MTT was added to each well. After the plates were incubated for 4 h, 100 μL formazan solubilization solution was added and left overnight. The absorbance was measured at the wavelength of 450 nm with a reference wavelength of 630 nm by microplate reader (Bio-Rad 680).

The activity of MG63 cells after 4 days culture was evaluated by measuring alkaline phosphatase (ALP) activity. The cells were washed with PBS (pH 7.4) for three times, detached with trypsin-EDTA, and lysed in 0.1% Triton X-100 by freezing and thawing for two cycles. The ALP activity of cells was measured using p-nitrophenyl phosphate (p-Npp) as the substrate (Sigma, St. Louis, MO, USA). After 30 min incubation at 37 °C the reaction was stopped by the addition of 1 $mol \cdot L^{-1}$ NaOH. The quantity of pNpp produced was measured at 410 nm using a microplate reader (Bio-RAD680) and the total protein content was measured using the BCA Protein Assay Kit (Sigma).

2.5. Statistical analysis

A software of origin 7.5 (Origin Lab Inc, USA) was used to analyze the obtained data. The values of weight increase and Ca/P molar ratio were averaged (n = 3). The results of cell experiment were expressed as means ± standard deviation (SD) (n = 5). Student's *t*-test was performed to determine the statistical significance and differences were considered statistically significant at $P<0.05$.

3. Results and discussion

3.1. Morphologies

Fig. 1 shows the various morphologies of mineralized electrospun PLGA and PLGA/gelatin nanofibers prepared by three mineralizing methods. It can be seen that the apatite deposited on the PLGA nanofiber via concentrated SBF method performed a microporous texture (Fig. 1(A, B, C)), whereas the apatite coating on the PLGA/gelatin nanofibrous scaffold showed a flaky texture (Fig. 1(D, E, F)). Compared with concentrated SBF method, the CaP apatite fabricated by supersaturated calcification solution method (Fig. 1(G–L)) and alternate soaking method (Fig. 1(M–R)) presented agglomerate feature. In addition, although the mineral apatite coated on the surface of PLGA and PLGA/gelatin nanofibrous scaffolds all increased with the increasing of soaking time, the amount of apatite on the surface of PLGA/gelatin nanofibrous scaffolds was more than that on the PLGA nanofibrous scaffolds. The reason might be that the carboxyl groups of the gelatin could attract and enrich Ca^{2+} ions in the solution, which could accelerate the nucleation and growth of apatite crystal [17]. Additionally, the adding of gelatin enhanced the hydrophilicity of scaffold, which is the reason why the apatite deposited only on the outer layer of the PLGA nanofibrous scaffolds but appeared both outer and inner of the PLGA/gelatin nanofibrous scaffolds.

3.2. Weight increase

To further study the effect of the methods on mineralization, the weight increase of CaP apatite coating was investigated, as listed in Table 2. It was shown that the weight increase of the supersaturated calcification solution method was the lowest and the alternate soaking method was the highest among the three methods. During the mineralization, the CaP crystal nuclear would form both in the solution and on the surface of the nanofibers, and the more apatite forming in the solution, the less apatite depositing on the surface of the nanofibers. In the supersaturated calcification solution method, when the pH of the solution was up to the critical value, a large amount of the apatite was rapidly appearing in the solution which consumed a large number of Ca^{2+} ions, so that less Ca^{2+} ions were left to form CaP apatite coating on the surface of nanofibers, thus the weight increase was lowest among the three methods. However, there was almost no white sediment in the $CaCl_2$ and Na_2HPO_4 solution for alternate soaking method, demonstrating that most of the Ca^{2+} ions were transforming into CaP coating instead of apatite being suspended in the solution. Therefore the weight increase of the alternate soaking method was highest because the efficiency of Ca transformation was the highest among the three methods. Otherwise, the weight of apatite deposited on the PLGA/gelatin nanofibers was higher than that on the PLGA nanofibers in three methods, which corresponded to the SEM images.

3.3. Composition of CaP coating

Table 3 shows the main elemental analysis results of mineralized PLGA and PLGA/gelatin nanofibers at different soaking time points through energy dispersive spectrum. It can be seen from Table 3 that elemental constituents of Ca and P on the surface of mineralized nanofibers increased with increasing soaking time, indicating that the surface of nanofibers was gradually covered by the CaP apatite, which coincided well with the SEM photographs in Fig. 1. In addition, according to the review of Boanini et al. [18], there are only several calcium orthophosphates that could be produced from liquid-state reaction: hydroxyapatite (HA) (Ca/P: 1.67), octacalcium phosphate (OCP) (Ca/P: 1.33), amorphous calcium phosphate (ACP) (Ca/P: 1.2–

Table 3
Molar ratios of Ca/P of minerals on the mineralized PLGA and PLGA/gelatin nanofibers.

Method	Time (h)	PLGA			PLGA/gelatin		
		Ca (at.%)	P (at.%)	Ca/P	Ca (at.%)	P (at.%)	Ca/P
Concentrated SBF solution method	1	2.77 ± 0.02	2.12 ± 0.04	1.31	2.26 ± 0.03	2.52 ± 0.01	0.90
	2	5.72 ± 0.01	5.28 ± 0.03	1.09	6.47 ± 0.01	6.18 ± 0.01	1.04
	3	12.43 ± 0.01	11.37 ± 0.01	1.09	15.89 ± 0.01	14.13 ± 0.02	1.12
Supersaturated calcification solution method	1	0.73 ± 0.01	0.79 ± 0.01	0.92	1.77 ± 0.01	1.60 ± 0.01	1.11
	2	1.28 ± 0.01	1.22 ± 0.02	1.05	2.59 ± 0.01	1.98 ± 0.02	1.31
	3	1.65 ± 0.02	1.31 ± 0.01	1.26	3.53 ± 0.02	2.79 ± 0.01	1.27
Alternate soaking method	1	3.20 ± 0.01	2.92 ± 0.02	1.10	3.58 ± 0.01	3.55 ± 0.01	1.01
	2	5.57 ± 0.01	4.67 ± 0.01	1.19	14.00 ± 0.02	12.12 ± 0.01	1.16
	3	16.95 ± 0.01	14.14 ± 0.02	1.20	17.40 ± 0.01	13.33 ± 0.01	1.31

2.2) and dicalcium phosphate dihydrate (DCPD) (Ca/P: 1.0). The present CaP coatings showed that the molar ratios of Ca/P were all less than 1.33, as listed in Table 3, which demonstrated that the apatite was not a single substance but a mixture of two or three calcium orthophosphates. There was no difference of Ca/P ratio between the apatite coating on the PLGA and PLGA/gelatin nanofibers because the components and structure of apatite were mainly related to the properties of solution.

In order to identify the CaP coating of mineralized PLGA and PLGA/gelatin nanofibers, the structure of products was characterized by using FT-IR and XRD. The FT-IR spectra of mineralized PLGA and PLGA/gelatin nanofibers are shown in Fig. 2. For concentrated SBF method (Fig. 2(A, B)), the strong absorption band at 1023 cm^{-1} was attributed to the $PO_4(\nu_3)$. The band at 1548 cm^{-1} and 870 cm^{-1} arise from CO_3^{2-} and a combination of CO_3^{2-} and HPO_4^{2-} [19–21], respectively. In addition, the characteristic absorption peaks appeared at 1645 cm^{-1}, 3494 cm^{-1} and 3534 cm^{-1} which corresponded to the bending and stretching of O–H in DCPD in Fig. 2(B) [10]. For supersaturated calcification method (Fig. 2(C, D)), only the bands at 1650 cm^{-1} (O–H) and 1555 cm^{-1} (CO_3^{2-}) in Fig. 2(C) and 1032 cm^{-1} (PO_4 ν_3) in Fig. 2(D) could be identified from the spectrum of PLGA and PLGA/gelatin nanofibers, which may relate to the little production of CaP apatite on the nanofiber surface [14,22,23]. For alternate soaking method (Fig. 2(E, F)), the band of the PO_4 (ν_3) was seen at 1035 cm^{-1}, CO_3^{2-} and CO_3^{2-} combined with HPO_4^{2-} were recorded at 1563 cm^{-1} and 876 cm^{-1}.

From the XRD patterns (Fig. 3) the composite could be clearly identified from the mixture of apatite deposited on the surface of mineralized PLGA and PLGA/gelatin nanofibers. As to concentrated SBF method, from Fig. 3(A) we can see that the peaks of DCPD (29°, 31.4° and 34.4°), HA (26°) and OCP (16.1°) appeared in the spectrum respectively [24–29]. Fig. 3(B) shows that the apatite also has the components of DCPD (11.4°, 20.8°, 29.2°, 31.4° and 34.4°), OCP (16.1° and 24.2°) and HA (26.1°, 32.3° and 35.1°), but the peaks were sharper than those in Fig. 3(A), indicating that the crystallization of CaP apatite on PLGA/gelatin nanofibers was higher than that on PLGA nanofibers. The results were similar to the report of Yang et al. [10]. From the XRD profiles of supersaturated calcification method (Fig. 3(C, D)), the mixtures were composed of DCPD, OCP and HA, and the content of HA was higher in the mixtures. It can also be seen that the broad peaks of CaP coating may be due to the little amount of mineral covered on the nanofibers (Fig. 1(C, D)). Compared with concentrated SBF method and supersaturated calcification solution method, the characteristic peaks of DCPD, OCP and HA were more and sharper in the XRD diffraction patterns of mineralized PLGA and PLGA/gelatin nanofibers prepared by alternate soaking method (Fig. 3(E,F)).

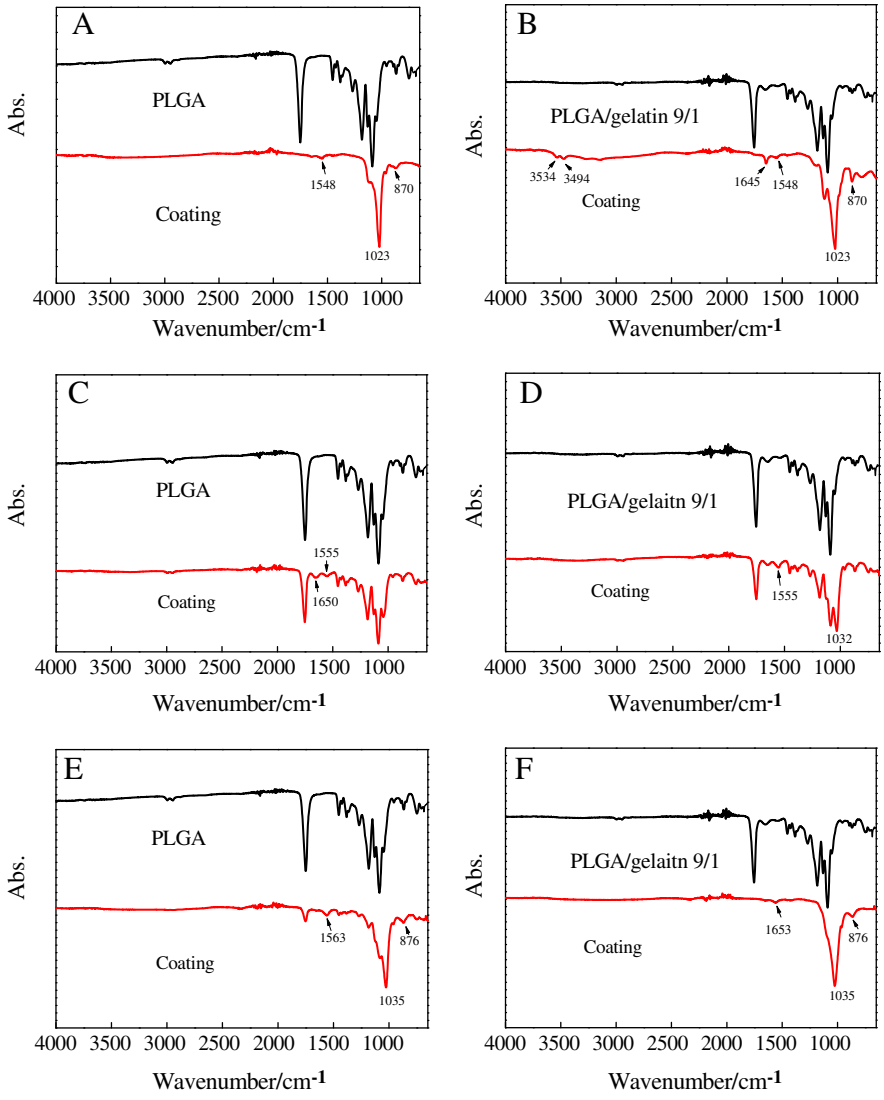

Fig. 2. FT-IR spectra of mineralized PLGA and PLGA/gelatin nanofibers. Concentrated SBF method: (A,B); supersaturated calcification solution method: (C,D); alternate soaking method: (E,F).

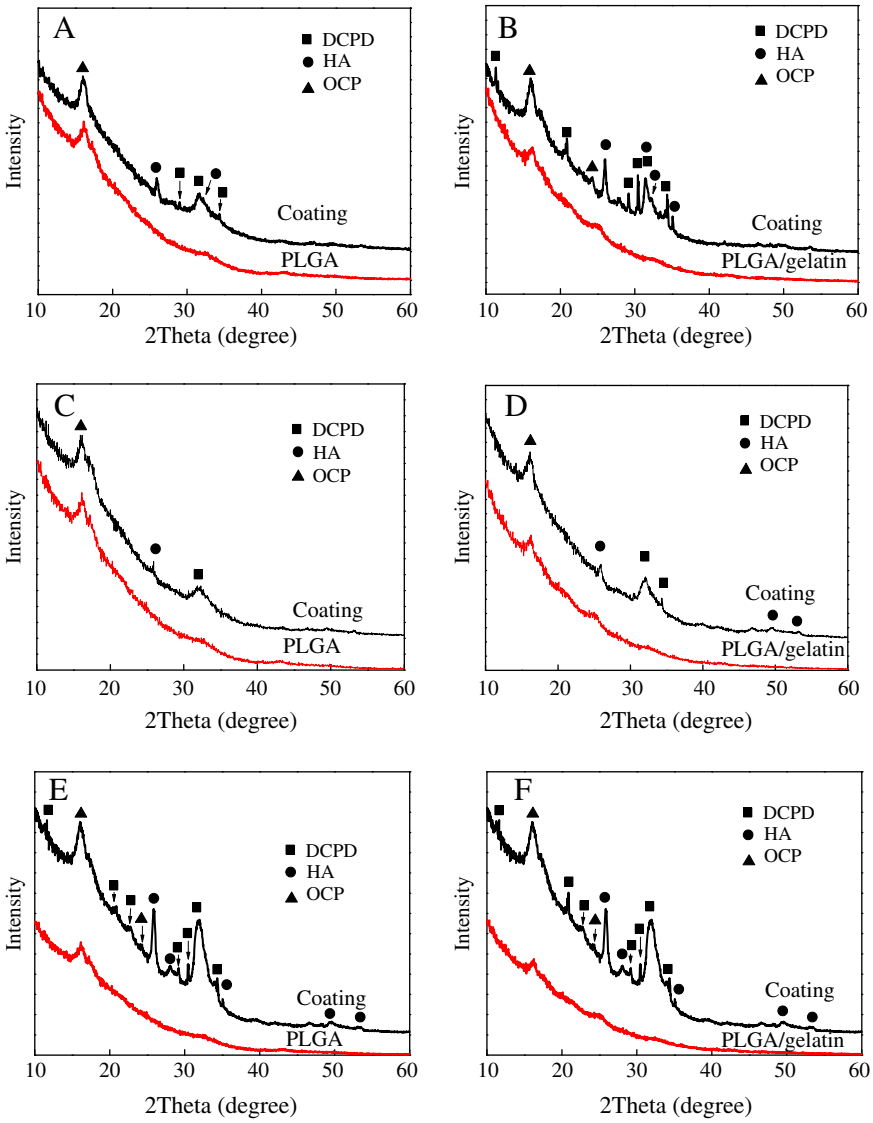

Fig. 3. XRD curves of mineralized PLGA and PLGA/gelatin nanofibers. Concentrated SBF method: (A,B); supersaturated calcification solution method: (C,D); alternate soaking method: (E,F).

3.4. Cell behavior

In order to estimate the biocompatibility of mineralized PLGA and PLGA/gelatin nanofibers fabricated by three mineralizing methods, MG63 cells were seeded onto mineralized PLGA and PLGA/gelatin nanofibrous scaffolds and co-cultured. The cell morphologies were analyzed by SEM, and cell proliferation and ALP activity were assayed by MTT and ALP assays. Fig. 4 presents the cell morphology on mineralized PLGA and PLGA/gelatin scaffolds after 1 and 4 days of cell culture. As shown in Fig. 4, after 1 day all the cells spread well on the surface of scaffolds, illustrating that the CaP coating showed positive for cell adhesion. After 4 days, more cells could be seen covering the mineralized scaffolds and some of them even infiltrated into the pore of the CaP coating, which reflected a good biocompatibility for mineralized scaffolds.

The proliferation of MG63 cells on mineralized PLGA and PLGA/gelatin nanofibrous scaffolds was studied at 1, 2 and 4 day, as shown in Fig. 5. On day 1 and day 4, there was no significant difference ($P>0.05$) in the absorption of mineralized groups and control group, only on day 2 that the absorption was different among the groups. It demonstrated that although the proliferation rates of cells in all groups were not the same in 4 days, the CaP coating fabricated by three methods did not present significant influence on the results of cell proliferation.

The ALP activity is believed as a marker of the early stages of osteogenic differentiation because it may increase with the maturation of osteoblasts. Fig. 6 revealed the ALP activity of MG63 cells cultured for 4 days on mineralized PLGA and PLGA/gelatin nanofibrous scaffolds. As can be seen in Fig. 6, excepting mineralized PLGA/gelatin nanofibers of alternate soaking, the ALP activity of the other mineralized nanofiber groups was a little higher than that of control groups but showed no significant difference ($P>0.05$), which showed that the difference of CaP apatite coating did not show much influence on the activity of MG63 cells.

4. Conclusions

In this study, mineralized PLGA and PLGA/gelatin electrospun nanofibrous scaffolds were fabricated through concentrated simulated body fluid method, supersaturated calcification method and alternated soaking method. The mineralized PLGA/gelatin nanofibers had the higher weight increase than PLGA nanofibers. The apatite yielded

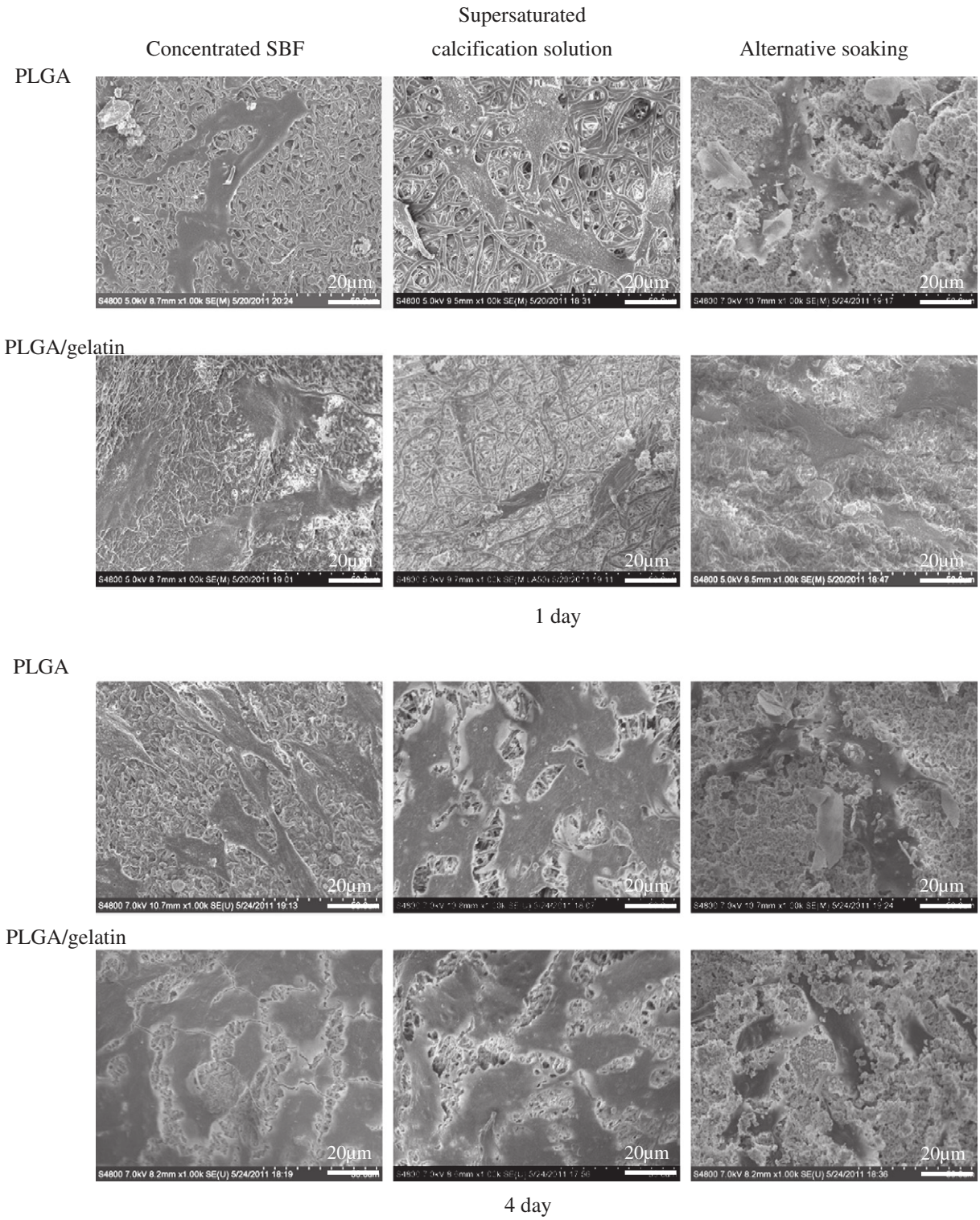

Fig. 4. Morphologies of MG63 cells on mineralized PLGA and PLGA/gelatin scaffolds after 1 and 4 days.

by three methods all contained DCPD, OCP and HA, and the main component of CaP coating from concentrated SBF method was DCPD, and HA content of coating was increasing in the other two methods. The morphologies and the components of CaP apatite coatings fabricated by three methods did not show much influence on adhesion, proliferation and activity of MG63 cells, thus the mineralized PLGA/gelatin nanofibers would be a suitable choice for bone tissue engineering among the experimental samples because of their high efficiency of mineralization.

Acknowledgments

This work is supported by the Innovation Foundation of Harbin City (no. 2011RFQXS099), the Postdoctoral Science-Research Developmental

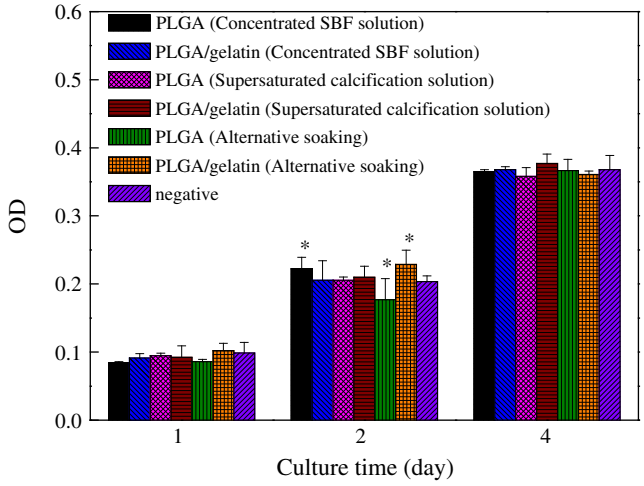

Fig. 5. MTT results of MG63 cells on mineralized PLGA and PLGA/gelatin nanofibrous scaffolds (* $P<0.05$).

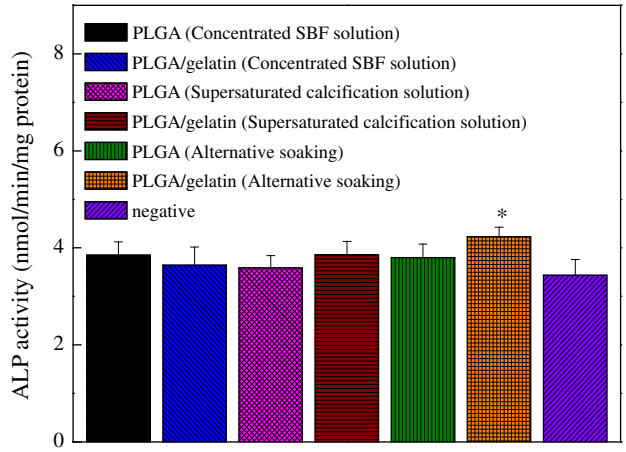

Fig. 6. ALP activity of MG63 cells cultured on mineralized PLGA and PLGA/gelatin nanofibrous scaffolds for 4 days (* $P<0.05$).

Foundation of Heilongjiang Province (no. LBH-Q09131), the Fundamental Research Funds for the Central Universities (no. HEUCFZ1123 and HEUCF201210008) and Natural Science Foundation of Heilongjiang Province (ZD201012).

References

[1] J.H. Jang, O. Castano, H.W. Kim, Adv. Drug Deliv. Rev. 61 (2009) 1065–1083.
[2] O.D. Schneider, F. Weber, T.J. Brunner, S. Loher, M. Ehrbar, P.R. Schmidlin, W.J. Stark, Acta Biomater. 5 (2009) 1775–1784.
[3] D.W. Hutmacher, Biomaterials 21 (2000) 2529–2543.
[4] X. Xin, M. Hussain, J.J. Mao, Biomaterials 28 (2007) 316–325.
[5] Y. Zhang, J.R. Venugopal, A. El-Turki, S. Ramakrishna, B. Su, C.T. Lim, Biomaterials 29 (2008) 4314–4322.
[6] F. Peng, X. Yu, M. Wei, Acta Biomater. 7 (2011) 2585–2592.
[7] D. Gupta, J. Venugopal, S. Mitra, V.R. Giri Dev, S. Ramakrishna, Biomaterials 30 (2009) 2085–2094.
[8] P. Jongwattanapisan, N. Charoenphandhu, N. Krishnamra, J. Thongbunchoo, I.-M. Tang, R. Hoonsawat, S.M. Smith, W. Pon-On, Mater. Sci. Eng. C 31 (2011) 290–299.
[9] D. Scharnweber, R. Born, K. Flade, S. Roessler, M. Stoelzel, H. Worch, Biomaterials 25 (2004) 2371–2380.
[10] F. Yang, J.G.C. Wolke, J.A. Jansen, J. Chem. Eng. 137 (2008) 154–161.
[11] S. Liao, R. Murugan, C.K. Chan, S. Ramakrishna, J. Mech. Behav. Biomed. Mater. 1 (2008) 252–260.
[12] T. Taguchi, Y. Muraoka, H. Matsuyama, A. Kishida, M. Akashi, Biomaterials 22 (2001) 53–58.
[13] P.Q. Ruhé, E.L. Hedberg-Dirk, N.T. Padron, P.H.M. Spauwen, J.A. Jansen, A.G. Mikos, Tissue Eng. 12 (2006) 789–800.
[14] P. Zhang, Z. Hong, T. Yu, X. Chen, X. Jing, Biomaterials 30 (2009) 58–70.
[15] M. Ngiam, S. Liao, A.J. Patil, Z. Cheng, C.K. Chan, S. Ramakrishna, Bone 45 (2009) 4–16.
[16] Z.X. Meng, Y.S. Wang, C. Ma, W. Zheng, L. Li, Y.F. Zheng, Mater. Sci. Eng. C 30 (2010) 1204–1210.
[17] S. Huang, K. Zhou, W. Zhu, B. Huang, Z. Li, J. Appl. Polym. Sci. 101 (2006) 1842–1847.
[18] E. Boanini, M. Gazzano, A. Bigi, Acta Biomater. 6 (2010) 1882–1894.
[19] C.Y. Zheng, S.J. Li, X.J. Tao, Y.L. Hao, R. Yang, L. Zhang, Mater. Sci. Eng. C 27 (2007) 824–831.
[20] X.D. Sun, Y.L. Zhou, J.Y. Ren, F.K. Cui, H.D. Li, Curr. Appl. Phys. 7S1 (2007) e75–e79.
[21] R. Alvareza, L.A. Evansa, P.J. Milhamb, M.A. Wilson, Geoderma 118 (2004) 245–260.
[22] J. Zhao, Y. Zhao, Q. Guan, G. Tang, Y. Zhao, X. Yuan, K. Yao, J. Appl. Polym. Sci. 119 (2011) 786–793.
[23] J. Chen, B. Chu, B.S. Hsiao, J. Biomed, Mater. Res. Part A 79A (2006) 307–317.
[24] C. Sekara, P. Kanchanaa, R. Nithyaselvi, E.K. Girija, Mater. Chem. Phys. 115 (2009) 21–27.
[25] L. He, Z. Feng, Mater. Lett. 61 (2007) 3923–3926.
[26] C.H. Hou, C.W. Chen, S.M. Hou, Y.T. Li, F.H. Lin, Biomaterials 30 (2009) 4700–4707.
[27] A. Rapacz-Kmitaa, C. Paluszkiewicza, A. losarczyk, Z. Paszkiewicz, J. Mol. Struct. 744–747 (2005) 653–656.
[28] R. Horváthová, L. Müller, A. Helebrant, P. Greil, F.A. Müller, Mater. Sci. Eng. C 28 (2008) 1414–1419.
[29] Z. Xu, K.G. Neoh, A. Kinshen, Mater. Sci. Eng. C 30 (2010) 822–826.